

# T Cell Receptor Protein Sequences and Sparse Coding: A Novel Approach to Cancer Classification

**Zahra Tayebi\***

*Department of Computer Science  
Georgia State University  
Atlanta, GA, USA*

ZTAYEBI1@STUDENT.GSU.EDU

**Sarwan Ali\***

*Department of Computer Science  
Georgia State University  
Atlanta, GA, USA*

SALI85@STUDENT.GSU.EDU

**Prakash Chourasia**

*Department of Computer Science  
Georgia State University  
Atlanta, GA, USA*

PCHOURASIA1@STUDENT.GSU.EDU

**Taslim Murad**

*Department of Computer Science  
Georgia State University  
Atlanta, GA, USA*

TMURAD2@STUDENT.GSU.EDU

**Murray Patterson<sup>+</sup>**

*Department of Computer Science  
Georgia State University  
Atlanta, GA, USA*

MPATTERSON30@GSU.EDU

## Abstract

Cancer is a complex disease characterized by uncontrolled cell growth and proliferation, which can lead to the development of tumors and metastases. The identification of the cancer type is crucial for selecting the most appropriate treatment strategy and improving patient outcomes. T cell receptors (TCRs) are essential proteins for the adaptive immune system, and their specific recognition of antigens plays a crucial role in the immune response against diseases, including cancer. The diversity and specificity of TCRs make them ideal for targeting cancer cells, and recent advancements in sequencing technologies have enabled the comprehensive profiling of TCR repertoires. This has led to the discovery of TCRs with potent anti-cancer activity and the development of TCR-based immunotherapies.

To analyze these complex biomolecules effectively, it is essential to represent them in a way that captures their structural and functional information. In this study, we investigate the use of sparse coding for the multi-class classification of TCR protein sequences with cancer categories as target labels. Sparse coding is a popular technique in machine learning that enables the representation of data with a set of informative features and can capture complex relationships between amino acids and identify subtle patterns in the sequence that might be missed by low-dimensional methods. We first compute the  $k$ -mers

---

\*. Equal Contribution

+. Corresponding Author

from the TCR sequences and then apply sparse coding to capture the essential features of the data. To improve the predictive performance of the final embeddings, we integrate domain knowledge regarding different types of cancer properties such as Human leukocyte antigen (HLA) types, gene mutations, clinical characteristics, immunological features, and epigenetic modifications. We then train different machine learning (linear and non-linear) classifiers on the embeddings of TCR sequences for the purpose of supervised analysis. Our proposed embedding method on a benchmark dataset of TCR sequences significantly outperforms the baselines in terms of predictive performance, achieving an accuracy of 99.8%. Our study highlights the potential of sparse coding for the analysis of TCR protein sequences in cancer research and other related fields.

## 1. Introduction

T cell receptors (TCRs) play a crucial role in the immune response by recognizing and binding to antigens presented by major histocompatibility complexes (MHCs) on the surface of infected or cancerous cells, Figure 1 (Shah et al., 2021). The specificity of TCRs for antigens is determined by the sequence of amino acids that make up the receptor, which is generated through a process of genetic recombination and somatic mutation. This enables T cells to produce a diverse repertoire of receptors capable of recognizing a wide range of antigens (Courtney et al., 2018).

MHC molecules bind to peptide fragments that originate from pathogens and present them on the cell surface. This allows for recognition by the corresponding T cells (Janeway Jr et al., 2001). TCR sequencing involves analyzing the DNA or RNA sequences that code for the TCR protein on T cells, and it can be used to identify changes in the TCR repertoire that occur in response to cancer, as well as to identify specific TCR sequences that are associated with particular types of cancer (Kidman et al., 2020; Robins et al., 2009). TCR protein sequences have become a focus of interest for cancer immunotherapy, as they can be used to engineer TCR-based therapies for cancer treatment (Eshhar et al., 1996).

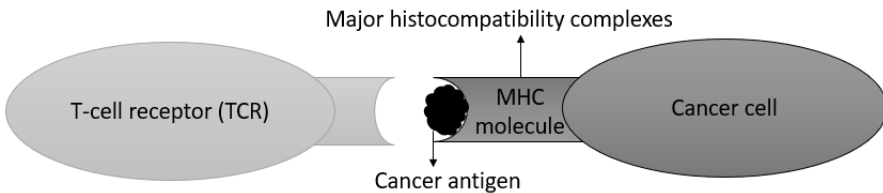


Figure 1: T-cells mount a targeted immune response against the invading pathogen of cancerous cells.

Embedding-based methods involve mapping sequences onto low-dimensional vector representations, which can then be used for various downstream analyses (Yang et al., 2020). Classification is a common application of embedding-based methods in protein sequence analysis. By representing protein sequences as embeddings, classifiers can be trained to predict the functional class of new, unlabeled protein sequences based on their similarity to the training data.(Hristescu and Farach-Colton, 1999; Iqbal et al., 2014). This tech-

nique can also be used to identify groups of related sequences with similar features, predict protein-protein interactions, and classify disease-causing mutations (Yang et al., 2020).

Embedding-based methods for protein sequence analysis face challenges in terms of generalizability and complexity (Alberts et al., 2002; Mikolov et al., 2013). However, deep learning methods, such as Convolutional Neural Networks (CNNs), Recurrent Neural Networks (RNNs), and transformer networks, have shown promise in addressing these challenges (Wang et al., 2019; Liu, 2017; Nambiar et al., 2020). By training on large and diverse datasets, deep learning models can improve generalization performance and make accurate predictions on new sequences. However, the quality and diversity of training data, model architecture, and optimization strategy are still critical factors influencing their performance (Min et al., 2021). Additionally, the interpretability of deep learning models for protein sequence analysis can be a challenge, requiring careful consideration and evaluation. Therefore, while deep learning can improve the generalizability of embedding-based methods, it may not entirely solve the problem.

In this study, we propose a multi-class classification approach using sparse coding for predicting cancer categories from TCR protein sequences. Sparse coding is a machine learning technique that finds a sparse representation of the input data using a dictionary of sparse basis functions (Olshausen and Field, 2004). By representing TCR protein sequences as sparse linear combinations of basis functions, we can capture the inherent structure and variation in the data, which can be used for accurate cancer classification. We preprocess the data by encoding the amino acid sequences as numerical vectors and perform sparse coding using a dictionary of  $k$ -mers, a commonly used basis function for analyzing biological sequences.

We evaluate the performance of our approach using various metrics and compare it to other state-of-the-art methods. Our results demonstrate that our method outperforms existing approaches in terms of classification predictive performance. The proposed approach possesses properties such as invariance, robustness to noise, interpretability, transferability, and flexibility.

The proposed approach possesses the following properties:

**Invariant property:** The invariant property is achieved in sparse coding by designing the basis vectors to be invariant to certain transformations of the input data. For example, in the case of protein sequences, the basis vectors may be designed to be invariant to amino acid substitutions or deletions. This means that even if small changes are made to the input sequence, the resulting sparse code will be relatively unchanged.

**Robustness to Noise:** Sparse coding-based embeddings are robust to noise in the input data because they learn a sparse representation that focuses on the most important features while ignoring the noise.

**Interpretability:** Sparse coding-based embeddings are interpretable because they learn a sparse representation that highlights the most important features of the protein sequences. This makes it possible to identify the specific amino acid residues that are most important for the function of a given protein.

**Transferability:** Sparse coding-based embeddings can be easily transferred to related tasks because the learned representation captures the most relevant information about the protein sequences.

**Flexibility:** Sparse coding-based embeddings can be adapted to different types of protein sequence data (e.g., protein families, domains, etc.) by training the model on a diverse set of sequences. This allows the model to learn a more general representation that can be applied to a wide range of problems.

In general, our contributions to this paper are the following:

1. We propose an efficient embedding method based on the idea of sparse coding and the power of  $k$ -mers to embed the T cell sequences into an alignment-free and fixed-length numerical representation.
2. Using the domain knowledge about different cancer types, we show that the predictive performance for supervised analysis can greatly be improved when combine with the sparse coding-based representation.
3. We show that the proposed embedding method gives near-perfect predictive performance and significantly outperforms all baselines in terms of classification accuracy. This behavior shows that although the length of T cell sequences is very small, they can still be distinguished from each other using efficient representation.

Given these considerations, we will continue as outlined below. In Section 2, we discuss the related work similar to the problem discussed in this paper. The proposed approach is given in Section 3. The detail regarding the dataset and experimental setup are shown in Section 4. The results for the proposed and baseline methods are reported in Section 5. Finally, the paper is concluded in Section 6.

## 2. Related Work

TCR sequencing data has been used to identify neoantigens that are specifically recognized by T cells, providing potential targets for immunotherapy (van den Berg et al., 2020). There are studies that used TCR sequencing and showed T cells play a prominent role in orchestrating the immune response to viral diseases, including SARS-CoV-2 infection (Gittelman et al., 2022) and can be used for measuring the adaptive immune response to SARS-CoV-2 (Elyanow et al., 2021). Furthermore, TCR sequencing data has been used to identify T-cell clones that are associated with tumor regression in response to immunotherapy (Lu et al., 2019). These studies have provided valuable insights into the mechanisms of immunotherapy and potential targets for therapy.

Classification methods have been shown to be beneficial for biological data analysis, such as protein sequence analysis in cancer classification (Hoadley et al., 2018). Support Vector Machines (SVM), Random Forest, and Logistic Regression are classification methods that can group protein sequences with similar features together, allowing researchers to identify subpopulations of protein sequences such as TCR sequences that may be associated with specific cancer types (Lin et al., 2019; Ru et al., 2019; Chen et al., 2020).

In one study, the authors used discriminant information of mutated genes in protein amino acid sequences for lung cancer classification (Sattar and Majid, 2019). They described

variations in amino acid sequences by statistical and physicochemical properties of amino acids and used these features to develop a lung cancer classification model (LCCM). Another study used SVM for TCR sequence classification to predict disease-free survival and overall survival in breast cancer patients (Bai et al., 2018).

Also, K-means classification showed promising results in protein sequence analysis in distinguishing colorectal cancer patients from normal individuals (Bae et al., 2021). Overall, classification methods are valuable tools for analyzing protein sequences for cancer-type detection and can provide important insights into the immune response to cancer.

Deep learning methods have been used to predict various protein properties, such as structure, function, stability, and interactions (Wan et al., 2019). Convolutional neural networks (CNNs) have been used to predict protein structure and function from amino acid sequences (Bileschi et al., 2019). Recurrent neural networks (RNNs) have been shown to be effective in modeling the temporal dependencies and long-range interactions in protein sequences (Zhang et al., 2021). A Universal Representation of Amino Acid Sequences (UniRep) is a method for embedding protein sequences using an RNN architecture (Alley et al., 2019). These methods have shown promising results in various biological data analysis tasks, including protein sequence analysis.

ProtVec stand for Protein Representation Vector for Protein Function Prediction is another method that proposed a distributed representation of protein sequences using word embedding techniques (Asgari and Mofrad, 2010). The method is a natural language processing technique and works based on training a skip-gram model on amino acid n-grams and using the learned embeddings to predict protein functions (Ostrovsy-Berman et al., 2021).

Another embedding method is SeqVec (Sequence-to-Vector) which is for embedding protein sequences using a hierarchical representation that captures both local and global features of the sequence (Heinzinger et al., 2019).

ESM (Evolutionary Scale Modeling) is another method that has a transformer-based architecture to encode protein sequences and refers to a protein representation method based on the ESM family of protein models (Lin et al., 2023). ESM is trained on a large dataset of protein sequences and structures to predict the 3D structure of a given protein sequence (Hu et al., 2022).

It is worth noting that the effectiveness of deep learning models in protein sequence analysis hinges on several factors, including the quality and diversity of the training data, the architecture of the model, and the optimization strategy used during training. However, as we discussed earlier, in this domain the interpretability of deep learning modes results is challenging, which can make it difficult to diagnose and address issues related to the model's generalizability. While deep learning can enhance the generalizability of embedding-based techniques for protein sequence analysis, it may not offer a complete solution and requires thorough evaluation and consideration.

### 3. Proposed Approach

Sparse coding is a machine-learning approach that has been used for generating feature representations for protein sequences. In sparse coding, the goal is to represent the input data (in this case, protein sequences) as a sparse linear combination of basis vectors. The

basis vectors are learned from the data and are designed to capture the most important features of the input data. We combine the idea of sparse coding with the power of  $k$ -mers to design an efficient embedding representation for the protein sequences. We also use domain knowledge to improve the information richness of the final embeddings. In this section, we start by describing the domain knowledge related to different cancers and how we are using them in our embeddings. We then discuss the proposed algorithm followed by a flow-chart-based discussion of the whole pipeline.

### 3.1. Incorporating Domain Knowledge

In this section, we give some examples of the additional property values for the four cancers we mentioned. There are many factors that can increase the risk of developing cancer including Human leukocyte antigen (HLA) types, gene mutations, clinical characteristics, immunological features, and epigenetic modifications.

#### HLA types:

HLA genes are a group of genes that encode proteins on the surface of cells. These proteins are responsible for presenting antigens, which are small molecules derived from pathogens or other foreign substances, to immune cells called T cells (Davies and Cohen, 1996). In the case of cancer, mutations in HLA genes can lead to changes in the presentation of antigens to T cells. This can result in the immune system failing to recognize and eliminate cancer cells, which can then grow and spread unchecked (Schaafsma et al., 2021).

#### Gene mutations:

In addition to HLA types, mutations in other genes can also contribute to the development and progression of cancer. For example, mutations in the tumor suppressor genes TP53 and BRCA1/2 are associated with an increased risk of several types of cancer, including breast, ovarian, and colorectal cancer (Peshkin et al., 2011) (Network et al., 2011) (Visvader, 2011).

#### Clinical characteristics:

Clinical characteristics such as age, gender, and family history can impact a person's risk of developing cancer (Rex et al., 1993). For example, certain types of cancer are more common in older individuals, while others are more common in younger people. Additionally, some types of cancer may be more prevalent in one gender over another. Furthermore, family history can play a role in cancer risk (Lee et al., 2019).

#### Immunological features:

Another important factor that can affect cancer outcomes is the immune system. Immune cells play a critical role in identifying and eliminating cancer cells (De Visser et al., 2006). In some cases, however, cancer cells may evade the immune system's surveillance and continue to grow and spread. The presence and activity of immune cells within tumors can impact cancer progression and response to treatment (Gonzalez et al., 2018).

## Epigenetic modifications:

Epigenetic modifications are another cancer factor, including DNA methylation, which plays an important role in the development and progression of cancer (Kelly et al., 2010). DNA methylation is a process by which a methyl group is added to the cytosine base of DNA, typically at cytosines followed by guanine residues (CpG) sites, resulting in gene silencing or altered gene expression (Maekita et al., 2006).

### 3.1.1. BREAST CANCER

Breast cancer is the second most common type of cancer worldwide. Many studies have shown a link between HLA and breast cancer (Liang et al., 2021). Specifically, the HLA-A2, HLA-B7, and HLA-DRB1\*15:01 alleles have been implicated in breast cancer susceptibility (Anagnostouli et al., 2014).

Mutations in several genes are another factor that has been associated with an increased risk of breast cancer, including Breast Cancer 1, (BRCA1), Breast Cancer 2 (BRCA2), tumor suppressor protein 53 (TP53), and PIK3CA (Johnson et al., 2007).

Clinical characteristics of breast cancer are another important factor that includes the size and grade (how different the cancer cells look) of the tumor compared to normal cells (Elston and Ellis, 1991). Further, Estrogen receptor-positive breast cancer cells and Progesterone receptor-positive breast cancer cells that have receptors that bind to the hormone estrogen and hormone progesterone respectively, can stimulate the growth of breast cancer (Sommer and Fuqua, 2001). The last clinical characteristic of breast cancer is the presence of Human Epidermal Growth Factor Receptor 2 (HER2) which is a protein that promotes cell growth and is found on the surface of some breast cancer cells (Loibl and Gianni, 2017).

One important immunological factor that affects the behavior and progression of the tumor is the infiltration of TILs, which are immune cells that can recognize and attack cancer cells (Salgado et al., 2015). Studies have shown that breast cancer patients with higher levels of TILs tend to have better clinical outcomes (Stanton and Disis, 2016).

Another key aspect of breast cancer immunology is the expression of immune checkpoint molecules such as Programmed Death 1 (PD-1), Programmed Death Ligand 1 (PD-L1), and cytotoxic T-lymphocyte–Associated Antigen 4 (CTLA-4) (Carosella et al., 2015). These molecules play a critical role in regulating the immune response and preventing the immune system from attacking healthy cells.

DNA methylation of BRCA1 and BRCA2 genes is an epigenetic modification that has shown promise as a potential biomarker for early detection, therapy monitoring, assessment of prognosis, or prediction of therapy response for breast cancer (Martens et al., 2009).

### 3.1.2. COLORECTAL CANCER

Colorectal cancer (CRC) is a type of cancer that starts in the colon or rectum. It often begins as a noncancerous growth called a polyp, which can turn cancerous over time. CRC is a complex disease that involves multiple genetic and environmental factors.

The HLA system is known to be involved in the development and progression of CRC. For example, the HLA-A11 and HLA-B44 alleles have been associated with a decreased risk

of CRC, while the HLA-DRB1\*04 allele has been associated with an increased risk ([Dunne et al., 2020](#)).

There are several gene mutations that have been linked to the development of colorectal cancer, including Adenomatous Polyposis Coli (APC), Kirsten Rat Sarcoma viral oncogene homolog (KRAS), Tumor Protein p53 (TP53), and B-Raf Proto-oncogene, serine/threonine kinase (BRAF). APC gene mutations are found in about 80% of sporadic (non-hereditary) colorectal cancers ([Fodde, 2002](#)).

The clinical characteristics of CRC include tumor location, stage, differentiation grade, and lymph node involvement. Another key player in the development and progression of CRC is the immune system. Several immunological features have been identified that are associated with CRC, including tumor-infiltrating lymphocytes (TILs) and the expression of immune checkpoint molecules such as PD-1, PD-L1, and CTLA-4 ([Rotte, 2019](#)).

As an epigenetic modification, DNA methylation of the Cyclin-Dependent Kinase Inhibitor 2A (CDKN2A) gene is a critical epigenetic modification that plays an important role in the development and progression of colorectal cancer ([Kim et al., 2010](#)).

### 3.1.3. LIVER CANCER

Liver cancer, also known as hepatocellular carcinoma, is a type of cancer that starts in the liver cells. Risk factors for liver cancer include chronic infection with hepatitis B or C viruses, heavy alcohol use, and certain genetic conditions ([Levrero, 2006](#)).

Studies have shown that individuals who have HLA-A2, HLA-B35, and HLA-DRB1\*01:01 may be at a higher risk of developing liver cancer, especially if they are also infected with hepatitis B or C viruses ([Mosaad, 2015](#)).

Also, gene mutations such as TP53, CTNNB1, Axin 1 (AXIN1), and AT-rich Interactive Domain-containing protein 1A (ARID1A) are thought to contribute to the development and progression of liver cancer by promoting abnormal cell growth and division ([Ozen et al., 2013](#)).

Clinical characteristics that are commonly used to assess the severity and prognosis of liver cancer include tumor size, number of nodules, portal vein invasion, and Alpha-Fetoprotein (AFP) levels. For example, larger tumors are generally associated with a worse prognosis and may be more difficult to treat ([Makuuchi et al., 1993](#)).

Moreover, Liver cancer immunological features that contribute to its progression and resistance to treatment can be the presence of TILs and the expression of immune checkpoint molecules such as PD-1, PD-L1, and CTLA-4, as well as high expression of immune regulatory genes such as Producing the Forkhead Box P3 (FOXP3) and Indoleamine 2,3-dioxygenase (IDO) ([Bufo et al., 2022](#)).

Research has shown that aberrant DNA methylation of CDKN2A, Methylguanine Methyltransferase (MGMT), and Glutathione S-Transferase Pi 1 (GSTP1) genes which is an epigenetic modification is commonly found in liver cancer and can contribute to the development and progression of the disease ([ZHU, 2005](#)).

### 3.1.4. UROTHELIAL CANCER

Urothelial cancer, also known as transitional cell carcinoma, is cancer that affects the cells lining the bladder, ureters, and renal pelvis ([Perez-Montiel et al., 2006](#)). There is some

evidence to suggest that certain HLA types such as HLA-A2 and HLA-B7 may be associated with an increased risk of developing urothelial cancer.

Further, there is evidence to suggest that mutations in certain genes, including Fibroblast Growth Factor Receptor 3 (FGFR3), TP53, Retinoblastoma (RB1), and PIK3CA, may play a role in the development of urothelial cancer (Smal et al., 2014).

The clinical characteristics of urothelial cancer are determined by several factors, including tumor stage, grade, and location. Immunological features of urothelial cancer can include the presence of TILs and the expression of immune checkpoint molecules such as PD-1, PD-L1, and CTLA-4. These are important immunological features of urothelial cancer that can impact prognosis and treatment options (Carosella et al., 2015).

DNA methylation of CDKN2A, p16, and Ras Association Domain Family Protein 1A (RASSF1A) genes is an important epigenetic modification that can play a critical role in the development and progression of urothelial cancer. DNA methylation patterns can be used as biomarkers for diagnosis, prognosis, and treatment for urothelial cancer (Florl et al., 1999).

### 3.2. Algorithmic Pseudocode

The code in Algorithm 1 defines a function *GenerateKmers* that takes in a sequence  $s \in S$  and an integer  $k$  and generates all possible  $k$ -mers of length  $k$  from the input sequence. The total number of  $k$ -mers, that can be generated for any sequence  $s$  of length  $n$  is the following:

$$\text{Total } k\text{-mers} = n - k + 1 \quad (1)$$

For ease of understanding, we use Python-like pseudocode in both Algorithm 1 and Algorithm 2.

---

**Algorithm 1** GenerateKmers

---

**Input:** sequence  $s$ ,  $k$   
**Output:** set of kmers

```

kmers ← []
for i ← 0 to len(s) - k + 1 do
    | kmers.append(s[i:i+k])
end
return kmers

```

---

The pseudocode to compute sparse coding +  $k$ -mers-based embedding is given in Algorithm 2. This algorithm takes a set of sequences  $S = \{s_1, s_2, \dots, N\}$  and  $k$ , where  $N$  is the number of sequences and  $k$  is the length of  $k$ -mers. The algorithm computed the sparse embedding by iterating over all sequences and computing the set of  $k$ -mers for each sequence. Then it iterates over all the  $k$ -mers, computes the one-hot encoding (OHE) based representation for each amino acid within a  $k$ -mer, and concatenates it with the OHE embeddings of other amino acids within the  $k$ -mer. Finally, the OHE embeddings for all  $k$ -mers within a sequence are concatenated to get the final sparse coding-based representation. To avoid the curse of dimensionality, we used Lasso regression as a dimensionality reduction technique (Ranstam and Cook, 2018). The objective function, which we used in lasso regression

is the following:

$$\min(\text{Sum of square residuals} + \alpha \times |slope|) \quad (2)$$

In the above equation, the  $\alpha \times |slope|$  is referred to as the penalty terms, which reduces the slope of insignificant features to zero. For experiments, we use  $k = 4$ , which is decided using the standard validation set approach.

---

**Algorithm 2** Sparse Coding Algorithm

---

**Input:** set of sequences  $S$ ,  $k$ -mers length  $k$

**Output:** SparseEmbedding

```

totValues = 21                                ▷ unique amino acid characters
final_sparse_embedding ← []
for i ← 0 to |S| do
    seq ← S[i]
    kmers ← GENERATEKMERS(seq, k)            ▷ generate set of  $k$ -mers
    encoded_kmers ← []
    for kmer in kmers do
        encodedVec ← np.zeros(totValuesk)      ▷  $21^3 = 9261$  dimensional vector
        for i, aa in enumerate(kmer) do
            pos ← i × totValuesk-i-1
            encodedVec[pos:pos+totValues] ← ONEHOTENCODING(aa)
        end
        encoded_kmers.append(encodedVec)
    end
    final_sparse_embedding.append(np.array(encoded_kmers).flatten())
end
SparseEmbedding ← LASSOREGRESSION(final_sparse_embedding)      ▷ dim. reduction
return SparseEmbedding

```

---

The same process repeated while we considered domain knowledge about cancer properties like HLA types, gene mutations, clinical characteristics, immunological features, and epigenetic modifications. That is, for each property, we generate a one-hot encoding-based representation, where the length of the vector equals the total number of possible property values. All OHE representations of the property values are concatenated in the end to get final representations for all properties that we consider from domain knowledge.

The resultant embeddings from Sparse coding (from Algorithm 2) and domain knowledge are concatenated in the end to get the final embedding. These embeddings are used to train machine-learning models for supervised analysis

### 3.3. Flow Chart

Figure 2 shows the flowchart overall embedding generation process. Initially, a TCR protein sequence associated with colorectal cancer is provided (Figure 2 (1-a)), To preserve the ordering information of the sequence,  $k$ -mers are generated for the sequence, as shown in (Figure 2 (1-b)). Subsequently, one-hot encoding (OHE) based representation is computed for each amino acid in each generated  $k$ -mer. The resulting one-hot encodings for each  $k$ -mer are combined together, as shown in Figure 2 (1-c to 1-d). Finally, the one-hot encoding

vectors of all generated  $k$ -mers are merged to create a final embedding vector (Figure 2 (1-e)). To avoid overfitting, Lasso regression is utilized as a dimensionality reduction technique, and the final merged one-hot vectors are passed through this method to generate final sparse coding-based representation, as shown in Figure 2 g. In parallel, the properties of colorectal cancer, such as HLA types and gene mutations, are taken into consideration. For each factor in each category of colorectal cancer properties, a one-hot encoding vector is generated (in Figure 2 2-a) two categories of cancer properties showed, but we considered all five different cancer properties). All the one-hot encoding vectors for the factors in each category of cancer properties are combined to create a single vector. Finally, the one-hot encoding vectors for all the cancer properties are merged to create the final embedding vectors, as depicted in Figure 2 (2-a to g). The resulting final embedding vectors are utilized as inputs to the classification methods to detect the related cancer type. This process is repeated for all other cancer types.

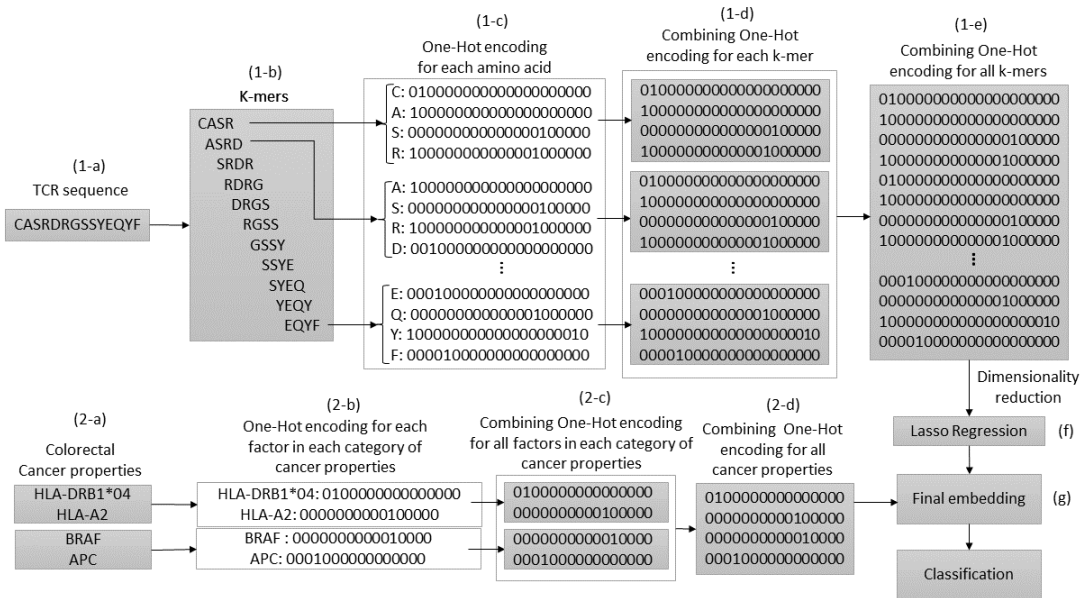


Figure 2: Flowchart of TCR sequence analysis

#### 4. Experimental Setup

In this section, we describe the detail related to the dataset followed by the description of baseline models, evaluation metrics, and data visualization. The experiments were performed on a system with an Intel(R) Core i5 processor @ 2.10GHz and a Windows 10 64 bit operating system, with 32 GB of memory. The implementation of the model was carried

out using Python and the code (and preprocessed dataset) has been made available online for reproducibility <sup>+</sup>.

#### 4.1. Dataset Statistics

We extract the spike sequence data from TCRdb which is a comprehensive database for T-cell receptor sequences with a powerful search function (Chen et al., 2021). TCRdb has collected over 130 projects and 8000 samples from public databases, which is a comprehensive TCR sequence resource to date. In this study, We identified and extracted the four most prevalent types of cancer based on their incidence rates. The extracted data contains 4 types of cancers within 23331 TCR sequences that are selected randomly by using the Stratified ShuffleSplit method to get the original proportion of the original data. Detailed statistics of the dataset can be seen in Table 1.

Our embedding generation method for this dataset uses TCR sequences, along with cancer names and specific cancer properties. Table 2 demonstrates examples of TCR sequences, which are short sequences of amino acids, along with cancer names and gene mutations for specific cancer types. The table includes four different cancer types with their corresponding gene mutations. The “Gene Mutation” column refers to the tumor suppressor gene mutations that can increase the risk of these types of cancer. For instance, mutations in the tumor suppressor genes TP53 and BRCA1/2 are associated with an increased risk of breast and colorectal cancer.

| Cancer Name | Number of Sequences | Sequence Length Statistics |      |         |
|-------------|---------------------|----------------------------|------|---------|
|             |                     | Min.                       | Max. | Average |
| Breast      | 4363                | 8                          | 20   | 14.2264 |
| Colorectal  | 10947               | 7                          | 26   | 14.5573 |
| Liver       | 3520                | 8                          | 20   | 14.3005 |
| Urothelial  | 4501                | 7                          | 24   | 14.6538 |
| Total       | 23331               | -                          | -    | -       |

Table 1: Dataset Statistics.

| Sequence        | Cancer Name | Gene Mutation              |
|-----------------|-------------|----------------------------|
| CASSRGQYEQYF    | Breast      | BRCA1, BRCA2, TP53, PIK3CA |
| CASSLEAGRAYEQYF | Colorectal  | APC, KRAS, TP53, BRAF      |
| CASSLGSGQETQYF  | Liver       | TP53, CTNNB1, AXIN1        |
| CASSGQGSSNSPLHF | Urothelial  | FGFR3, TP53, RB1, PIK3CA   |

Table 2: An example of sequences for different cancer types, Breast, Colorectal, Liver, and Urothelial along with their respective gene mutations.

<sup>+</sup>. Accessible in the published version

## 4.2. Baseline Models

To evaluate our proposed system we used various baselines and the details of each baseline method are as follows,

### 4.2.1. ONE HOT ENCODING (OHE) ([KUZMIN ET AL., 2020](#))

OHE generates binary vectors to represent the sequences in numerical form. For every alphabet in a sequence, it creates binary vectors of size equal to the number of all possible alphabets and assigns a 1 to the corresponding character's location while all others have 0 value. These vectors are concatenated to produce the final numerical embedding of the sequence.

### 4.2.2. SPIKE2VEC ([ALI AND PATTERSON, 2021](#))

Spike2Vec is a method to convert bio-sequences into numerical form for enabling ML-based classification of the sequences. It generates the embedding of a sequence by counting its  $k$ -mers occurrences, as  $k$ -mers are known to retain the ordering information of the sequence. For a sequence, its  $k$ -mers consists of consecutive substrings of length  $k$  driven from the sequence. For instance, a sequence of length  $N$  will have  $N - k + 1$   $k$ -mers. For our experiments, we used  $k = 3$ .

### 4.2.3. PWM2VEC ([ALI ET AL., 2022](#))

PWM2Vec is another technique to get numerical embeddings of the biological sequences following the  $k$ -mers concept, however, rather than using the  $k$ -mers frequencies, it assigns weights to each amino acid of the  $k$ -mers and employs these weights to generate the embeddings. Assigning weights enables to preserve the position-wise relative importance of the amino acids in a  $k$ -mer, along with retaining the ordering information. The weights are determined using a position weight matrix (PWM). For our experiments, we used  $k = 3$ .

### 4.2.4. SPACED $k$ -MERS ([SINGH ET AL., 2017](#))

The embeddings generated using  $k$ -mers suffer from sparsity and curse of dimensionality challenges which affect the analytical performance negatively. To tackle these issues, the concept of spaced  $k$ -mers is introduced, which refers to a set of non-contiguous substrings of length  $k$  and is known as  $g$ -mers. For a given sequence, spaced  $k$ -mers first compute the  $g$ -mers of the sequence and then extract  $k$ -mers from these  $g$ -mers to form an embedding. We use  $k = 4$  and  $g = 9$  in our experiments.

### 4.2.5. AUTO ENCODER ([XIE ET AL., 2016](#))

In this approach, a neural network is used to get the numerical features of the bio-sequence data. It follows the autoencoder architecture where the encoder module is optimized to get the embeddings. The encoder performs a non-linear transformation of data from space  $X$  to a low dimensional numerical feature space  $Z$ . We are using two layered autoencoder networks, along with an ADAM optimizer and MSE loss function, in our experiments.

#### 4.2.6. WASSERSTEIN DISTANCE GUIDED REPRESENTATION LEARNING (WDGRL) ([SHEN ET AL., 2018](#))

WDGRL employs a neural network to extract the numerical features by optimizing the Wasserstein distance (WD) between the source and target distributions. It falls in the category of unsupervised domain adoption techniques. For a given sequence, its one-hot encoded vector is generated and this vector is passed on to the WDGRL to get the final embeddings.

#### 4.2.7. STRING KERNEL ([FARHAN ET AL., 2017](#))

String kernel works by designing a kernel matrix to generate the numerical vectors for the bio-sequences. Given two sequences, it measures the similarity between them by determining the number of matched and mismatched  $k$ -mers. Once the kernel matrix is created, it is passed to kernel PCA to get the principal components-based feature embeddings.

#### 4.2.8. PROTEIN BERT ([BRANDES ET AL., 2022](#))

This approach employs a pre-trained language model to perform the classification of protein sequences. This model has introduced novel architectural elements to deal with long protein sequences efficiently. It captures both global and local representations within protein sequences. This end-to-end technique is using the transformer to do classification by taking the protein sequences as input.

#### 4.2.9. SEQVEC ([HEINZINGER ET AL., 2019](#))

SeqVec (Sequence-to-Vector) technique uses a language model, known as ELMO (Embeddings from Language Models) ([Sarzynska-Wawer et al., 2021](#)), to obtain the feature vectors of protein sequences. This model is trained using unlabeled data from UniRef50 and it generates embeddings depending on the context of the word.

### 4.3. Classifiers & Evaluation Metrics

Various ML classifiers are used to perform the classification task and those classifiers are, Support Vector Machine (SVM), Naive Bayes (NB), Multi-Layer Perceptron (MLP), K-Nearest Neighbors (KNN) with  $k = 3$ , Random Forest (RF), Logistic Regression (LR), and Decision Tree (DT). We used a 70-30% train-test split based on stratified sampling to do classification. From the training set, we use 10% data as a validation set for hyperparameter tuning. The results are computed 5 times and the average results are reported.

Furthermore, the performance of all the baselines and our proposed method is evaluated using different evaluation metrics, and those metrics are, average accuracy, precision, recall, F1 (weighted), F1 (macro), Receiver Operator Characteristic Curve (ROC), Area Under the Curve (AUC), and training runtime metrics. Moreover, the one-vs-rest approach is used to convert the binary evaluation metrics to multi-class ones.

### 4.4. Data Visualization

In order to see if there is any natural (hidden) clustering in the data, we use t-distributed stochastic neighbor embedding (t-SNE) ([Van and Hinton, 2008](#)), which maps input se-

quences to 2D representation. Particularly in the natural sciences, t-SNE is well-liked because of its ability to handle vast volumes of data and its usage for dimensionality reduction while maintaining the structure of the data. The t-SNE plots for different embedding methods are shown in Figure 3 for One hot encoding (OHE), Spike2Vec, PWM2Vec, Spaced Kmer, Autoencoder, and Sparse Coding, respectively. In general, we can observe that OHE, Spike2Vec, PWM2Vec, and Autoencoder show a smaller set of groups for different cancer types. However, the Spaced  $k$ -mers show a very scattered representation of data. Moreover, the proposed Sparse Coding approach does not show any scattered representation, hence preserving the overall structure better.

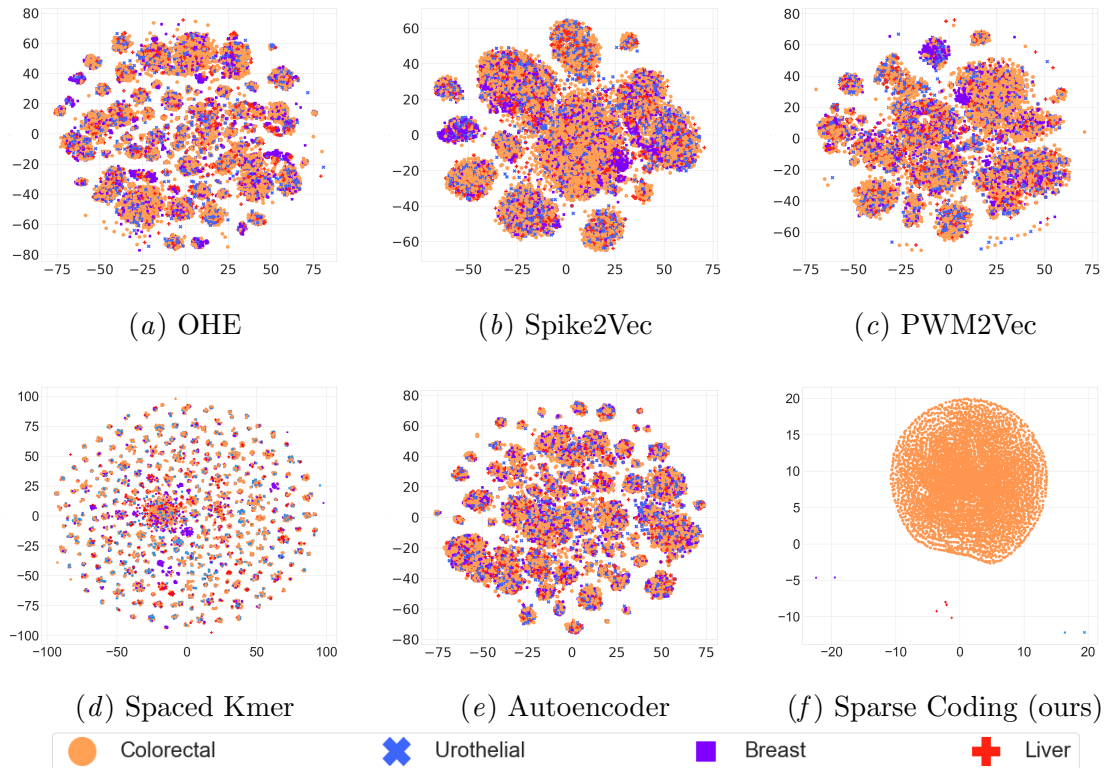


Figure 3: t-SNE plots for different feature embedding methods. The figure is best seen in color.

## 5. Results And Discussion

This section discusses the classification results achieved by our proposed system and the baselines against various ML models. The results for different evaluation metrics are reported in Table 3. We can observe that, our proposed technique (Sparse Coding) is outperforming all the feature-engineering-based baseline models (OHE, Spike2Vec, PWM2Vec, Spaced  $k$ -mers) for every evaluation metric except training runtime. For instance, Sparse

Coding obtains 48.5% more accuracy than OHE, 55.8% more than Spike2Vec, 58.4% more than PWM2Vec, and 48.6% more than Spaced  $k$ -mers using LR classifier. These results imply that the feature embeddings generated by the Sparse Coding method retain more information about the biological sequences in terms of classification performance as compared to the feature-engineering-based baselines.

Similarly, our technique is also better performing than the neural network-based baselines (WDGRL, Autoencoder). For example, the WDGRL approach has 53.03% less accuracy than the Sparse Coding and Autoencoder achieves 53.83% lower accuracy than Sparse Coding corresponding to the SVM classifier. This indicates that the feature vectors generated from the neural network-based techniques are not efficient for performing classification tasks as compared to the Sparse Coding-based feature vectors. Note that SVM is yielding the best results among all the classifiers corresponding to WDGRL and Autoencoder methods.

Likewise, our method is also portraying better predictive results as compared to the kernel-based baseline (String Kernel), like it has 53.83% more accuracy than String Kernel using the SVM model. This yet again shows that Sparse Coding is creating more efficient numerical vectors for protein sequences.

Furthermore, we also compared Sparse Coding performance with the pre-trained models (SeqVec and Protein Bert), and the results illustrate that Sparse Coding is outperforming them in terms of all the evaluation metrics except the training runtime. This is an indication that the pre-trained models are not able to generalize well to our dataset therefore they are exhibiting lower predictive performance.

As it is obvious in our dataset some classes have fewer examples than the other classes and we are dealing with a class imbalance problem in the data. This can cause problems for classification models because they may become biased towards the majority class, leading to poor performance in predicting the minority class. To confirm if our classifiers are biased toward a single class, we examined various metrics like precision, recall, F1 (weighted, Macro), and ROC-AUC which are sensitive to class imbalance. All of these evaluation metrics showed that the combination of Sparse Coding with all seven classification methods outperformed the baseline methods and ensured that our results are reliable and can be used to inform future research in the field.

We can also notice that Sparse Coding is taking longer training runtime as compared to most of the baseline methods, however, it has tremendous performance improvement over all the baseline methods in terms of every other evaluation metric. As our aim is to design an efficient feature extraction model for getting higher classification results, so Sparse Coding has been shown to achieve that goal.

### 5.1. Statistical Significance of Results

We assessed the statistical significance of our computed results by conducting a Student's t-test and examining the  $p$ -values. To compute the  $p$ -values, we used the average and standard deviation (SD) of 5 runs. Our analysis revealed that the majority of the  $p$ -values were less than 0.05, which indicates the statistical significance of the results. This is likely due to the low SD values observed in our study.

| Embeddings            | Algo. | Acc. $\uparrow$ | Prec. $\uparrow$ | Recall $\uparrow$ | F1 (Weig.) $\uparrow$ | F1 (Macro) $\uparrow$ | ROC AUC $\uparrow$ | Train Time (sec.) $\downarrow$ |
|-----------------------|-------|-----------------|------------------|-------------------|-----------------------|-----------------------|--------------------|--------------------------------|
| OHE                   | SVM   | 0.5101          | 0.5224           | 0.5101            | 0.4073                | 0.3152                | 0.5592             | 790.5622                       |
|                       | NB    | 0.2036          | 0.3533           | 0.2036            | 0.0917                | 0.1213                | 0.5107             | 1.0560                         |
|                       | MLP   | 0.4651          | 0.4368           | 0.4651            | 0.4370                | 0.3714                | 0.5764             | 221.0638                       |
|                       | KNN   | 0.4464          | 0.4044           | 0.4464            | 0.4100                | 0.3354                | 0.5617             | 7.2748                         |
|                       | RF    | 0.5156          | 0.5003           | 0.5156            | 0.4521                | 0.3751                | 0.5824             | 18.7857                        |
|                       | LR    | 0.5143          | 0.5241           | 0.5143            | 0.4327                | 0.3492                | 0.5701             | 61.8512                        |
| Spike2Vec             | DT    | 0.4199          | 0.4129           | 0.4199            | 0.4160                | 0.3616                | 0.5737             | 1.0607                         |
|                       | SVM   | 0.4309          | 0.4105           | 0.4309            | 0.4157                | 0.3543                | 0.5711             | 19241.67                       |
|                       | NB    | 0.2174          | 0.3535           | 0.2174            | 0.1931                | 0.2081                | 0.5221             | 6.1309                         |
|                       | MLP   | 0.4191          | 0.4081           | 0.4191            | 0.4128                | 0.3490                | 0.5671             | 227.2146                       |
|                       | KNN   | 0.4397          | 0.4105           | 0.4397            | 0.4087                | 0.3400                | 0.5673             | 40.4765                        |
|                       | RF    | 0.5183          | 0.5078           | 0.5183            | 0.4519                | 0.3738                | 0.5836             | 138.6850                       |
| PWM2Vec               | LR    | 0.4404          | 0.4189           | 0.4404            | 0.4251                | 0.3626                | 0.5728             | 914.7739                       |
|                       | DT    | 0.4510          | 0.4307           | 0.4510            | 0.4365                | 0.3745                | 0.5805             | 40.3568                        |
|                       | SVM   | 0.4041          | 0.3760           | 0.4041            | 0.3836                | 0.3138                | 0.5452             | 10927.61                       |
|                       | NB    | 0.2287          | 0.3758           | 0.2287            | 0.2109                | 0.2220                | 0.5273             | 23.9892                        |
|                       | MLP   | 0.4053          | 0.3820           | 0.4053            | 0.3888                | 0.3226                | 0.5467             | 253.6387                       |
|                       | KNN   | 0.4454          | 0.3890           | 0.4454            | 0.3930                | 0.3069                | 0.5475             | 10.2005                        |
| Spaced $k$ -mers      | RF    | 0.4994          | 0.4745           | 0.4994            | 0.4370                | 0.3548                | 0.5716             | 126.5780                       |
|                       | LR    | 0.4143          | 0.3861           | 0.4143            | 0.3937                | 0.3237                | 0.5484             | 991.8051                       |
|                       | DT    | 0.4339          | 0.4078           | 0.4339            | 0.4140                | 0.3496                | 0.5636             | 34.9344                        |
|                       | SVM   | 0.5109          | 0.5221           | 0.5109            | 0.4095                | 0.3143                | 0.5582             | 824.215                        |
|                       | NB    | 0.2157          | 0.3713           | 0.2157            | 0.1296                | 0.1510                | 0.5144             | 0.1883                         |
|                       | MLP   | 0.4524          | 0.4203           | 0.4524            | 0.4236                | 0.3550                | 0.5663             | 207.685                        |
| Auto Encoder          | KNN   | 0.4527          | 0.4078           | 0.4527            | 0.4132                | 0.3351                | 0.5607             | 3.3905                         |
|                       | RF    | 0.5204          | 0.5233           | 0.5204            | 0.4294                | 0.3393                | 0.5679             | 41.3547                        |
|                       | LR    | 0.5121          | 0.5053           | 0.5121            | 0.4318                | 0.3441                | 0.5674             | 25.7664                        |
|                       | DT    | 0.4006          | 0.4009           | 0.4006            | 0.4006                | 0.3433                | 0.5629             | 14.2816                        |
|                       | SVM   | 0.4597          | 0.2113           | 0.4597            | 0.2896                | 0.1575                | 0.5000             | 14325.09                       |
|                       | NB    | 0.2601          | 0.3096           | 0.2601            | 0.2682                | 0.2317                | 0.5005             | 0.3491                         |
| WDGRL                 | MLP   | 0.3996          | 0.3132           | 0.3996            | 0.3226                | 0.2252                | 0.5017             | 110.76                         |
|                       | KNN   | 0.3791          | 0.3245           | 0.3791            | 0.3329                | 0.2445                | 0.5068             | 5.9155                         |
|                       | RF    | 0.4457          | 0.3116           | 0.4457            | 0.3023                | 0.1792                | 0.5003             | 76.2106                        |
|                       | LR    | 0.4520          | 0.3170           | 0.4520            | 0.2982                | 0.1712                | 0.5004             | 98.5936                        |
|                       | DT    | 0.3131          | 0.3119           | 0.3131            | 0.3124                | 0.2525                | 0.5016             | 25.1653                        |
|                       | SVM   | 0.4677          | 0.2188           | 0.4677            | 0.2981                | 0.1593                | 0.5000             | 15.34                          |
| String Kernel         | NB    | 0.4469          | 0.3231           | 0.4469            | 0.3397                | 0.2213                | 0.5105             | 0.0120                         |
|                       | MLP   | 0.4749          | 0.4659           | 0.4749            | 0.3432                | 0.2184                | 0.5163             | 15.43                          |
|                       | KNN   | 0.3930          | 0.3415           | 0.3930            | 0.3523                | 0.2626                | 0.5156             | 0.698                          |
|                       | RF    | 0.4666          | 0.4138           | 0.4666            | 0.3668                | 0.2578                | 0.5255             | 5.5194                         |
|                       | LR    | 0.4676          | 0.2187           | 0.4676            | 0.2980                | 0.1593                | 0.4999             | 0.0799                         |
|                       | DT    | 0.3604          | 0.3606           | 0.3604            | 0.3605                | 0.2921                | 0.5304             | 0.2610                         |
| Protein Bert          | SVM   | 0.4597          | 0.2113           | 0.4597            | 0.2896                | 0.1575                | 0.5000             | 2791.61                        |
|                       | NB    | 0.3093          | 0.3067           | 0.3093            | 0.3079                | 0.2463                | 0.4980             | 0.2892                         |
|                       | MLP   | 0.3287          | 0.3045           | 0.3287            | 0.3121                | 0.2402                | 0.4963             | 125.66                         |
|                       | KNN   | 0.3683          | 0.3106           | 0.3683            | 0.3229                | 0.2330                | 0.5001             | 3.1551                         |
|                       | RF    | 0.4469          | 0.3251           | 0.4469            | 0.3041                | 0.1813                | 0.5010             | 55.3158                        |
|                       | LR    | 0.4451          | 0.3080           | 0.4451            | 0.3026                | 0.1787                | 0.5000             | 2.0463                         |
| SeqVec                | DT    | 0.3073          | 0.3082           | 0.3073            | 0.3077                | 0.2502                | 0.4998             | 17.0352                        |
|                       | -     | 0.2624          | 0.4223           | 0.2624            | 0.1947                | 0.209                 | 0.5434             | 987.354                        |
|                       | SVM   | 0.432           | 0.422            | 0.432             | 0.415                 | 0.377                 | 0.530              | 100423.017                     |
|                       | NB    | 0.192           | 0.530            | 0.192             | 0.086                 | 0.117                 | 0.505              | 77.271                         |
|                       | MLP   | 0.428           | 0.427            | 0.428             | 0.427                 | 0.371                 | 0.580              | 584.382                        |
|                       | KNN   | 0.432           | 0.385            | 0.432             | 0.391                 | 0.306                 | 0.544              | 227.877                        |
| Sparse Cod-ing (ours) | RF    | 0.525           | 0.524            | 0.525             | 0.445                 | 0.360                 | 0.576              | 350.057                        |
|                       | LR    | 0.420           | 0.414            | 0.420             | 0.417                 | 0.356                 | 0.571              | 90626.797                      |
|                       | DT    | 0.397           | 0.397            | 0.397             | 0.397                 | 0.344                 | 0.562              | 2626.082                       |
|                       | SVM   | 0.9980          | 0.9950           | 0.9980            | 0.9960                | 0.9970                | 0.9950             | 16965.48                       |
|                       | NB    | 0.9970          | 0.9960           | 0.9970            | 0.9970                | 0.9960                | 0.9980             | 404.2999                       |
|                       | MLP   | 0.9950          | 0.9950           | 0.9950            | 0.9950                | 0.9947                | 0.9956             | 5295.811                       |
| Sparse Cod-ing (ours) | KNN   | <b>0.9990</b>   | <b>0.9990</b>    | <b>0.9990</b>     | <b>0.9990</b>         | <b>0.9989</b>         | <b>0.9991</b>      | 346.7334                       |
|                       | RF    | <b>0.9990</b>   | <b>0.9970</b>    | <b>0.9990</b>     | <b>0.9950</b>         | 0.9950                | 0.9960             | 1805.593                       |
|                       | LR    | <b>0.9990</b>   | 0.9940           | <b>0.9990</b>     | 0.9980                | 0.9980                | 0.9940             | <b>134.8503</b>                |
|                       | DT    | 0.9970          | 0.9980           | 0.9970            | 0.9960                | 0.9980                | 0.9970             | 449.9304                       |

Table 3: Classification results (averaged over 5 runs) for different evaluation metrics. The best values are shown in bold.

## 6. Conclusion

In this study, we proposed a novel approach for cancer classification using sparse coding and TCR protein sequences. Our approach first transformed TCR sequences into feature vectors using  $k$ -mers and then generate embedding using sparse coding. We also incorporate domain knowledge about different cancer properties in the final embeddings to enhance their predictive performance. We then trained several multi-class classifiers on the sparse codes generated by the learned dictionary, achieving state-of-the-art performance on a benchmark dataset of TCR sequences compared to several baseline methods. Our method achieves the maximum 99.9% accuracy, and 99.9% F1 and ROC AUC scores for this data classification. The use of sparse coding allows us to capture the essential features of biological data, which can ultimately aid in the development of more effective cancer therapies. The invariant and robust properties of sparse coding make it a promising technique for the analysis of biological sequences. Further research can investigate the potential of sparse coding for other types of biological data analysis and explore ways to optimize the method for different cancer types and TCR sequences. One potential avenue for future research is to explore the use of alternative basis functions for sparse coding, beyond  $k$ -mers. For example, other types of basis functions, such as position weight matrices or hidden Markov models, could be investigated for their suitability in capturing the structure of TCR protein sequences. Furthermore, it would be interesting to investigate the potential of using TCR protein sequences in combination with other types of data, such as gene expression or epigenetic data, to improve cancer classification and gain a more comprehensive understanding of the underlying biology of cancer. Exploring the scalability of the current method on multi-million sequences is another potential future direction.

## References

Bruce Alberts, Alexander Johnson, Julian Lewis, Martin Raff, Keith Roberts, and Peter Walter. The shape and structure of proteins. In *Molecular Biology of the Cell. 4th edition.* Garland Science, 2002.

Sarwan Ali and Murray Patterson. Spike2vec: An efficient and scalable embedding approach for covid-19 spike sequences. In *IEEE International Conference on Big Data*, pages 1533–1540, 2021.

Sarwan Ali, Babatunde Bello, Prakash Chourasia, Ria Thazhe Punathil, Yijing Zhou, and Murray Patterson. Pwm2vec: An efficient embedding approach for viral host specification from coronavirus spike sequences. *MDPI Biology*, 2022.

Ethan C Alley, Grigory Khimulya, Surojit Biswas, Mohammed AlQuraishi, and George M Church. Unified rational protein engineering with sequence-based deep representation learning. *Nature methods*, 16(12):1315–1322, 2019.

Maria Anagnostouli, Georgios Anagnostoulis, Serafeim Katsavos, Maria Panagiotou, Evangelia Kararizou, and Panagiota Davaki. Hla-drb1\* 15: 01 and epstein–barr virus in a multiple sclerosis patient with psoriasis, nasopharyngeal and breast cancers. lessons for

possible hidden links for autoimmunity and cancer. *Journal of the Neurological Sciences*, 339(1-2):26–31, 2014.

Ehsaneddin Asgari and Mohammad RK Mofrad. Protvec: A continuous distributed representation of biological sequences. *Computer Science*, 10(11):e0141287, 2010.

Jin Hee Bae, Minwoo Kim, JS Lim, and Zong Woo Geem. Feature selection for colon cancer detection using k-means clustering and modified harmony search algorithm. *Mathematics*, 9(5):570, 2021.

Fang Bai, Chuanchao Wei, Peng Zhang, Dexi Bi, Meixin Ge, Qing Chen, Yijun Jia, Yunshu Lu, and Kejin Wu. Use of peripheral lymphocytes and support vector machine for survival prediction in breast cancer patients. *Translational Cancer Research*, 7(4), 2018.

Maxwell L Bileschi, David Belanger, Drew Bryant, Theo Sanderson, Brandon Carter, D Sculley, Mark A DePristo, and Lucy J Colwell. Using deep learning to annotate the protein universe. *BioRxiv*, page 626507, 2019.

Nadav Brandes, Dan Ofer, Yam Peleg, Nadav Rappoport, and Michal Linial. ProteinBERT: a universal deep-learning model of protein sequence and function. *Bioinformatics*, 38(8):2102–2110, 02 2022.

Sandra Bufo, Artur Zimmermann, Sarina Ravens, Immo Prinz, Laura Elisa Buitrago-Molina, Robert Geffers, Norman Woller, Florian Kühnel, Steven R Talbot, Fatih Noyan, et al. Pd-1/ctla-4 blockade leads to expansion of cd8+ pd-1int tils and results in tumor remission in experimental liver cancer. *Liver Cancer*, 2022.

Edgardo D Carosella, Guillaume Ploussard, Joel LeMaoult, and Francois Desgrandchamps. A systematic review of immunotherapy in urologic cancer: evolving roles for targeting of ctla-4, pd-1/pd-l1, and hla-g. *European urology*, 68(2):267–279, 2015.

Cheng Chen, Qingmei Zhang, Bin Yu, Zhaomin Yu, Patrick J Lawrence, Qin Ma, and Yan Zhang. Improving protein-protein interactions prediction accuracy using xgboost feature selection and stacked ensemble classifier. *Computers in Biology and Medicine*, 123:103899, 2020.

Si-Yi Chen, Tao Yue, Qian Lei, and An-Yuan Guo. Tcrdb: a comprehensive database for t-cell receptor sequences with powerful search function. *Nucleic Acids Research*, 49(D1):D468–D474, 2021.

Adam H Courtney, Wan-Lin Lo, and Arthur Weiss. Tcr signaling: mechanisms of initiation and propagation. *Trends in biochemical sciences*, 43(2):108–123, 2018.

David R Davies and Gerson H Cohen. Interactions of protein antigens with antibodies. *Proceedings of the National Academy of Sciences*, 93(1):7–12, 1996.

Karin E De Visser, Alexandra Eichten, and Lisa M Coussens. Paradoxical roles of the immune system during cancer development. *Nature reviews cancer*, 6(1):24–37, 2006.

Margaret R Dunne, James J Phelan, Adriana J Michielsen, Aoife A Maguire, Cara Dunne, Petra Martin, Sinead Noonan, Miriam Tosetto, Robert Geraghty, David Fennelly, et al. Characterising the prognostic potential of hla-dr during colorectal cancer development. *Cancer Immunology, Immunotherapy*, 69:1577–1588, 2020.

Christopher W Elston and Ian O Ellis. Pathological prognostic factors in breast cancer. i. the value of histological grade in breast cancer: experience from a large study with long-term follow-up. *Histopathology*, 19(5):403–410, 1991.

Rebecca Elyanow, Thomas M Snyder, Sudeb C Dalai, Rachel M Gittelman, Jim Boonyaratanaakornkit, Anna Wald, Stacy Selke, Mark H Wener, Chihiro Morishima, Alex L Greninger, et al. T-cell receptor sequencing identifies prior sars-cov-2 infection and correlates with neutralizing antibody titers and disease severity. *medRxiv*, 2021.

Zelig Eshhar, Nathan Bach, Cheryl J Fitzer-Attas, Gidi Grosse, Joseph Lustgarten, Tova Waks, and Daniel G Schindler. The t-body approach: potential for cancer immunotherapy. In *Springer seminars in immunopathology*, volume 18, pages 199–209. Springer, 1996.

Muhammad Farhan, Juvaria Tariq, Arif Zaman, Mudassir Shabbir, and Imdad Ullah Khan. Efficient approximation algorithms for strings kernel based sequence classification. *Advances in neural information processing systems*, 30, 2017.

Andrea R Florl, R Löwer, BJ Schmitz-Dräger, and WA Schulz. Dna methylation and expression of line-1 and herv-k provirus sequences in urothelial and renal cell carcinomas. *British journal of cancer*, 80(9):1312–1321, 1999.

R Fodde. The apc gene in colorectal cancer. *European journal of cancer*, 38(7):867–871, 2002.

Rachel M Gittelman, Enrico Lavezzo, Thomas M Snyder, H Jabran Zahid, Cara L Carty, Rebecca Elyanow, Sudeb Dalai, Ilan Kirsch, Lance Baldo, Laura Manuto, et al. Longitudinal analysis of t cell receptor repertoires reveals shared patterns of antigen-specific response to sars-cov-2 infection. *JCI insight*, 7(10), 2022.

Hugo Gonzalez, Catharina Hagerling, and Zena Werb. Roles of the immune system in cancer: from tumor initiation to metastatic progression. *Genes & development*, 32(19–20):1267–1284, 2018.

Michael Heinzinger, Ahmed Elnaggar, Yu Wang, Christian Dallago, Dmitrii Nечаев, Florian Matthes, and Burkhard Rost. Modeling aspects of the language of life through transfer-learning protein sequences. *BMC bioinformatics*, 20(1):1–17, 2019.

Katherine A Hoadley, Christina Yau, Toshinori Hinoue, Denise M Wolf, Alexander J Lazar, Esther Drill, Ronglai Shen, Alison M Taylor, Andrew D Cherniack, Vésteinn Thorsson, et al. Cell-of-origin patterns dominate the molecular classification of 10,000 tumors from 33 types of cancer. *Cell*, 173(2):291–304, 2018.

Gabriela Hristescu and Martin Farach-Colton. Cluster-preserving embedding of proteins. Technical report, Technical Report 99-50, Computer Science Department, Rutgers University, 1999.

Mingyang Hu, Fajie Yuan, Kevin K Yang, Fusong Ju, Jin Su, Hui Wang, Fei Yang, and Qiuyang Ding. Exploring evolution-based &-free protein language models as protein function predictors. *arXiv preprint arXiv:2206.06583*, 2022.

Muhammad Javed Iqbal, Ibrahima Faye, Brahim Belhaouari Samir, and Abas Md Said. Efficient feature selection and classification of protein sequence data in bioinformatics. *The Scientific World Journal*, 2014, 2014.

Charles A Janeway Jr, Paul Travers, Mark Walport, and Mark J Shlomchik. The major histocompatibility complex and its functions. In *Immunobiology: The Immune System in Health and Disease. 5th edition*. Garland Science, 2001.

Nichola Johnson, Olivia Fletcher, Claire Palles, Matthew Rudd, Emily Webb, Gabrielle Sellick, Isabel dos Santos Silva, Valerie McCormack, Lorna Gibson, Agnes Fraser, et al. Counting potentially functional variants in brca1, brca2 and atm predicts breast cancer susceptibility. *Human molecular genetics*, 16(9):1051–1057, 2007.

Theresa K Kelly, Daniel D De Carvalho, and Peter A Jones. Epigenetic modifications as therapeutic targets. *Nature biotechnology*, 28(10):1069–1078, 2010.

Joel Kidman, Nicola Principe, Mark Watson, Timo Lassmann, Robert A Holt, Anna K Nowak, Willem Joost Lesterhuis, Richard A Lake, and Jonathan Chee. Characteristics of tcr repertoire associated with successful immune checkpoint therapy responses. *Frontiers in Immunology*, 11:587014, 2020.

Myoung Sook Kim, Juna Lee, and David Sidransky. Dna methylation markers in colorectal cancer. *Cancer and Metastasis Reviews*, 29:181–206, 2010.

Kiril Kuzmin et al. Machine learning methods accurately predict host specificity of coronaviruses based on spike sequences alone. *Biochemical and Biophysical Research Communications*, 533(3):553–558, 2020.

Andrew Lee, Nasim Mavaddat, Amber N Wilcox, Alex P Cunningham, Tim Carver, Simon Hartley, Chantal Babb de Villiers, Angel Izquierdo, Jacques Simard, Marjanka K Schmidt, et al. Boadicea: a comprehensive breast cancer risk prediction model incorporating genetic and nongenetic risk factors. *Genetics in Medicine*, 21(8):1708–1718, 2019.

M Levrero. Viral hepatitis and liver cancer: the case of hepatitis c. *Oncogene*, 25(27): 3834–3847, 2006.

H Liang, T Lu, H Liu, and L Tan. The relationships between hla-a and hla-b genes and the genetic susceptibility to breast cancer in guangxi. *Russian Journal of Genetics*, 57: 1206–1213, 2021.

Jianying Lin, Hui Chen, Shan Li, Yushuang Liu, Xuan Li, and Bin Yu. Accurate prediction of potential druggable proteins based on genetic algorithm and bagging-svm ensemble classifier. *Artificial intelligence in medicine*, 98:35–47, 2019.

Zeming Lin, Halil Akin, Roshan Rao, Brian Hie, Zhongkai Zhu, Wenting Lu, Nikita Smetanin, Robert Verkuil, Ori Kabeli, Yaniv Shmueli, et al. Evolutionary-scale prediction of atomic-level protein structure with a language model. *Science*, 379(6637):1123–1130, 2023.

Xueliang Liu. Deep recurrent neural network for protein function prediction from sequence. *arXiv preprint arXiv:1701.08318*, 2017.

Sibylle Loibl and Luca Gianni. Her2-positive breast cancer. *The Lancet*, 389(10087):2415–2429, 2017.

Yong-Chen Lu, Li Jia, Zhili Zheng, Eric Tran, Paul F Robbins, and Steven A Rosenberg. Single-cell transcriptome analysis reveals gene signatures associated with t-cell persistence following adoptive cell therapy gene signatures associated with t-cell persistence. *Cancer immunology research*, 7(11):1824–1836, 2019.

Takao Maekita, Kazuyuki Nakazawa, Mami Mihara, Takeshi Nakajima, Kimihiko Yanaoka, Mikitaka Iguchi, Kenji Arii, Atsushi Kaneda, Tetsuya Tsukamoto, Masaë Tatematsu, et al. High levels of aberrant dna methylation in helicobacter pylori–infected gastric mucosae and its possible association with gastric cancer risk. *Clinical Cancer Research*, 12(3):989–995, 2006.

Masatoshi Makuuchi, Tomoo Kosuge, Tadatoshi Takayama, Susumu Yamazaki, Tohoru Kakazu, Shinichi Miyagawa, and Seiji Kawasaki. Surgery for small liver cancers. In *Seminars in surgical oncology*, volume 9, pages 298–304. Wiley Online Library, 1993.

John WM Martens, Astrid L Margossian, Manfred Schmitt, John Foekens, and Nadia Harbeck. Dna methylation as a biomarker in breast cancer. *Future oncology*, 5(8):1245–1256, 2009.

Tomas Mikolov, Kai Chen, Greg Corrado, and Jeffrey Dean. Efficient estimation of word representations in vector space. *arXiv preprint arXiv:1301.3781*, 2013.

Seonwoo Min, Seunghyun Park, Siwon Kim, Hyun-Soo Choi, Byunghan Lee, and Sungroh Yoon. Pre-training of deep bidirectional protein sequence representations with structural information. *IEEE Access*, 9:123912–123926, 2021.

YM Mosaad. Clinical role of human leukocyte antigen in health and disease. *Scandinavian journal of immunology*, 82(4):283–306, 2015.

Ananthan Nambiar, Maeve Hefflin, Simon Liu, Sergei Maslov, Mark Hopkins, and Anna Ritz. Transforming the language of life: transformer neural networks for protein prediction tasks. In *Proceedings of the 11th ACM international conference on bioinformatics, computational biology and health informatics*, pages 1–8, 2020.

Cancer Genome Atlas Research Network et al. Integrated genomic analyses of ovarian carcinoma. *Nature*, 474(7353):609, 2011.

Bruno A Olshausen and David J Field. Sparse coding of sensory inputs. *Current opinion in neurobiology*, 14(4):481–487, 2004.

Miri Ostrovsky-Berman, Boaz Frankel, Pazit Polak, and Gur Yaari. Immune2vec: Embedding b/t cell receptor sequences in n using natural language processing. *Frontiers in immunology*, 12:680687, 2021.

Cigdem Ozen, Gokhan Yildiz, Alper Tunga Dagcan, Dilek Cevik, Aysegul Ors, Umur Kelles, Hande Topel, and Mehmet Ozturk. Genetics and epigenetics of liver cancer. *New biotechnology*, 30(4):381–384, 2013.

Delia Perez-Montiel, Paul E Wakely, Ondrej Hes, Michal Michal, and Saul Suster. High-grade urothelial carcinoma of the renal pelvis: clinicopathologic study of 108 cases with emphasis on unusual morphologic variants. *Modern Pathology*, 19(4):494–503, 2006.

Beth N Peshkin, Michelle L Alabek, and Claudine Isaacs. Brca1/2 mutations and triple negative breast cancers. *Breast disease*, 32(1-2):25–33, 2011.

Jonas Ranstam and JA Cook. Lasso regression. *Journal of British Surgery*, 105(10):1348–1348, 2018.

Douglas K Rex, Glen A Lehman, Thomas M Ulbright, Jennefer J Smith, David C Pound, Robert H Hawes, Debra J Helper, Maurits J Wiersema, Carl D Langefeld, and Wei Li. Colonic neoplasia in asymptomatic persons with negative fecal occult blood tests: influence of age, gender, and family history. *American Journal of Gastroenterology (Springer Nature)*, 88(6), 1993.

Harlan S Robins, Paulo V Campregher, Santosh K Srivastava, Abigail Wacher, Cameron J Turtle, Orsalem Kahsai, Stanley R Riddell, Edus H Warren, and Christopher S Carlson. Comprehensive assessment of t-cell receptor  $\beta$ -chain diversity in  $\alpha\beta$  t cells. *Blood, The Journal of the American Society of Hematology*, 114(19):4099–4107, 2009.

Anand Rotte. Combination of cta-4 and pd-1 blockers for treatment of cancer. *Journal of Experimental & Clinical Cancer Research*, 38:1–12, 2019.

Xiaoqing Ru, Lihong Li, and Quan Zou. Incorporating distance-based top-n-gram and random forest to identify electron transport proteins. *Journal of Proteome Research*, 18(7):2931–2939, 2019.

Roberto Salgado, Carsten Denkert, S Demaria, N Sirtaine, F Klauschen, Giancarlo Pruneri, S Wienert, Gert Van den Eynden, Frederick L Baehner, Frederique Pénault-Llorca, et al. The evaluation of tumor-infiltrating lymphocytes (tils) in breast cancer: recommendations by an international tils working group 2014. *Annals of oncology*, 26(2):259–271, 2015.

Justyna Sarzynska-Wawer, Aleksander Wawer, Aleksandra Pawlak, Julia Szymanowska, Izabela Stefaniak, Michal Jarkiewicz, and Lukasz Okruszek. Detecting formal thought disorder by deep contextualized word representations. *Psychiatry Research*, 304:114135, 2021.

Mohsin Sattar and Abdul Majid. Lung cancer classification models using discriminant information of mutated genes in protein amino acids sequences. *Arabian Journal for Science and Engineering*, 44:3197–3211, 2019.

Evelien Schaafsma, Chloe M Fugle, Xiaofeng Wang, and Chao Cheng. Pan-cancer association of hla gene expression with cancer prognosis and immunotherapy efficacy. *British Journal of Cancer*, 125(3):422–432, 2021.

Kinjal Shah, Amr Al-Haidari, Jianmin Sun, and Julhash U Kazi. T cell receptor (tcr) signaling in health and disease. *Signal transduction and targeted therapy*, 6(1):412, 2021.

Jian Shen, Yanru Qu, Weinan Zhang, and Yong Yu. Wasserstein distance guided representation learning for domain adaptation. In *AAAI conference on artificial intelligence*, 2018.

Ritambhara Singh, Arshdeep Sekhon, Kamran Kowsari, Jack Lanchantin, Beilun Wang, and Yanjun Qi. Gakco: a fast gapped k-mer string kernel using counting. In *Joint European Conference on Machine Learning and Knowledge Discovery in Databases*, pages 356–373, 2017.

MP Smal, AI Rolevich, SL Polyakov, SA Krasny, and RI Goncharova. Fgfr3 and tp53 mutations in a prospective cohort of belarusian bladder cancer patients. *Experimental oncology*, 2014.

Stephanie Sommer and Suzanne AW Fuqua. Estrogen receptor and breast cancer. In *Seminars in cancer biology*, volume 11, pages 339–352. Elsevier, 2001.

Sasha E Stanton and Mary L Disis. Clinical significance of tumor-infiltrating lymphocytes in breast cancer. *Journal for immunotherapy of cancer*, 4:1–7, 2016.

L. Van and G. Hinton. Visualizing data using t-sne. *Journal of Machine Learning Research (JMLR)*, 9(11), 2008.

Joost H van den Berg, Bianca Heemskerk, Nienke van Rooij, Raquel Gomez-Eerland, Samira Michels, Maaike van Zon, Renate de Boer, Noor AM Bakker, Annelies Jorritsma-Smit, Marit M van Buuren, et al. Tumor infiltrating lymphocytes (til) therapy in metastatic melanoma: boosting of neoantigen-specific t cell reactivity and long-term follow-up. *Journal for immunotherapy of cancer*, 8(2), 2020.

Jane E Visvader. Cells of origin in cancer. *Nature*, 469(7330):314–322, 2011.

Fangping Wan, Yue Zhu, Hailin Hu, Antao Dai, Xiaoqing Cai, Ligong Chen, Haipeng Gong, Tian Xia, Dehua Yang, Ming-Wei Wang, et al. Deepcpi: a deep learning-based framework for large-scale in silico drug screening. *Genomics, proteomics & bioinformatics*, 17(5):478–495, 2019.

Lei Wang, Hai-Feng Wang, San-Rong Liu, Xin Yan, and Ke-Jian Song. Predicting protein-protein interactions from matrix-based protein sequence using convolution neural network and feature-selective rotation forest. *Scientific reports*, 9(1):9848, 2019.

Junyuan Xie, Ross Girshick, and Ali Farhadi. Unsupervised deep embedding for clustering analysis. In *International conference on machine learning*, pages 478–487, 2016.

Xiaodi Yang, Shiping Yang, Qinmengge Li, Stefan Wuchty, and Ziding Zhang. Prediction of human-virus protein-protein interactions through a sequence embedding-based machine learning method. *Computational and structural biotechnology journal*, 18:153–161, 2020.

Jianlei Zhang, Yukun Zeng, and Binil Starly. Recurrent neural networks with long term temporal dependencies in machine tool wear diagnosis and prognosis. *SN Applied Sciences*, 3:1–13, 2021.

Jing De ZHU. The altered dna methylation pattern and its implications in liver cancer. *Cell research*, 15(4):272–280, 2005.